Conducting antireflection coatings with low polarization dependent loss for telecommunication applications

J. A. Dobrowolski[1], Joseph E. Ford[2], Brian T. Sullivan[3], Liping Lu[3], and Norman R. Osborne[3]

[1]*Institute for Microstructural Sciences, National Research Council of Canada, Ottawa, Ontario, Canada K1A 0R6.*
[2]*Electrical & Computer Engineering Department, University of California San Diego, 9500 Gilman Drive, La Jolla, CA 92093-0407*
[3]*Iridian Spectral Technologies, 1500 Montreal Road, Ottawa, Ontario K1A 0R6*
George.Dobrowolski@NRC.CA, jeford@ucsd.edu, brian.sullivan@iridian.ca

Abstract: Conducting optical coatings for the visible light range are commonly made of Indium Tin Oxide (ITO), but ITO is unsuitable for near-infrared telecommunications wavelengths because it can become absorptive after extended illumination. In this paper we show an alternative approach which uses conventional coating materials to create either non-conducting or conducting antireflection (AR) coatings that are effective over a fairly broad spectral region ($\lambda_{long}/\lambda_{short} \approx 1.40$) and also usable for a wide range of angles of incidence (0-38º, or 0-55º) in the telecom wavelength range. Not only is the transmittance of windows treated with such coatings quite high, but they can be made to have extreme polarization independence (low polarization dependent loss values). A number of such coating designs are presented in the paper. A prototype of one of the conducting AR coating designs was fabricated and the measurements were found to be in reasonable agreement with the calculated performance. Such AR coatings should be of interest for telecommunication applications and especially for anti-static hermetic packaging of MEMS devices such as optical switches.

OCIS codes: (310.1210) Antireflection; (060.1810) Couplers, switches, and multiplexers

References and Links

1. D.T. Neilson, R. Frahm, P. Kolodner, R.R. Bolle, C. , J. Kim, A. Papazian, C. Nuzman, A. Gasparyan, N. Basavanhally, V. Aksyuk and J. Gates, "256x256 Port Optical Cross-Connect Subsystem," IEEE Journal of Lightwave Technology **22**, 1499-1509 (2004).
2. J.E. Ford, V.A. Aksyuk, D.J. Bishop and J.A. Walker, " Wavelength add/drop switching using tilting micromirrors.," IEEE Journal of Lightwave Technology **17**, 904-911 (1999).
3. W.F. Wu and B.S. Chiou, "Effect of annealing on electrical and optical properties of RF magnetron sputtered indium tin oxide films," Applied Surface Science **68**, 497-504 (1993).
4. A. Thelen and H. König, "Zur Entspiegelung von elektrisch leitender Glasoberflächen," in *Ergebnisse der Hochvakuumtechnik und Physik dünner Schichten* **1**, (ed. M. Auwärter) (Wissenschafliche Verlagsgesellschaft MBH, Stuttgart, 1957), pp. 237-240.
5. R.E. Laird, J.D. Wolfe and C.K. Carniglia, "Durable conductive anti-reflection coatings for glass and plastic substrates," in *Proc. of the 39th Ann. Tech. Conf.,* Philadelphia, PA, Society of Vacuum Coaters (1996).
6. J. Strumpfel, G. Beister, D. Schulze, M. Kammer and S. Rehn, "Reactive dual magnetron sputtering of oxides for large area production of optical multilayers," in *Proc. of the 40th Ann. Tech. Conf.,* New Orleans, LA, Society of Vacuum Coaters (1997).
7. R. Wang and C.C. Lee, "Design of antireflection coating using Indium Tin Oxide (ITO) film prepared by Ion Assisted Deposition (IAD)," in *Proc. of the 42nd Ann. Tech. Conf.,* Chicago, I1, Society of Vacuum Coaters (1999).

8. B.T. Sullivan and J.A. Dobrowolski, "Implementation of a numerical needle method for thin-film design," Appl. Opt. **35**, 5484-5492 (1996).
9. B.T. Sullivan, G. Clarke, T. Akiyama, N. Osborne, M. Ranger, J.A. Dobrowolski, L. Howe, A. Matsumoto, Y. Song and K. Kikuchi, "High-rate automated deposition system for the manufacture of complex multilayer coatings," Appl. Opt. **39**, 157-167 (2000).
10. J.A. Dobrowolski, S. Browning, M. Jacobson and M. Nadal, "Topical Meeting on Optical Interference Coatings (OIC'2001): manufacturing problem," Appl. Opt. **41**, 3039-3052 (2002).
11. B.T. Sullivan and K.L. Byrt, "Metal/dielectric transmission interference filters with low reflectance. II. Experimental results," Appl. Opt. **34**, 5684-5694 (1995).

1. Introduction

In telecommunications there is a growing use of micro-electromechanical systems (MEMS) components that handle optical data transmitted by fiber-optics [1, 2]. Such devices often operate in the near infrared wavelength range from about 1260 to 1625 nm, and especially in the 1260-1360 nm and 1525-1625 nm spectral bands. Various optical coatings are required for MEMS devices, including reflecting coatings, beam splitters, band pass filters of various kinds and anti-reflection (AR) coatings. In general, it is important that these coatings do not significantly polarize light at non-normal angles of incidence. To quantify this, a quantity known as the polarization dependent loss (*PDL*) is typically used. In terms of transmittance, PDL_T [dB] is equal to $-10\log(T_s/T_p)$, where p and s denote light polarized parallel and perpendicular to the plane of incidence, respectively.

Figure 1 shows a schematic with certain elements of a typical MEMS based optical switch sealed in a hermetic housing. Here the light that is to be modulated is introduced into the device via an optical fiber. A grin lens then directs it towards an electrostatically controlled primary mirror that reflects it towards one of several secondary mirrors that, in turn, direct it in certain directions towards a window in the housing. The window can be made of sapphire, fused silica or other similar materials that are transparent in the near-IR. Because in some MEMS devices the light needs to pass through the window up to four times (eight surfaces) it is important that the surfaces of the windows carry efficient AR coatings.

The electrostatically controlled mirrors contained within the housing are sensitive to, and must be shielded from, external electrical fields. For this reason, the casings of MEMS devices are usually made of Kovar or other metallic materials. However, the windows must be made of near-IR transparent dielectric materials. This gives rise to two problems. First, surface charges that accumulate on the window surface may interfere with the proper

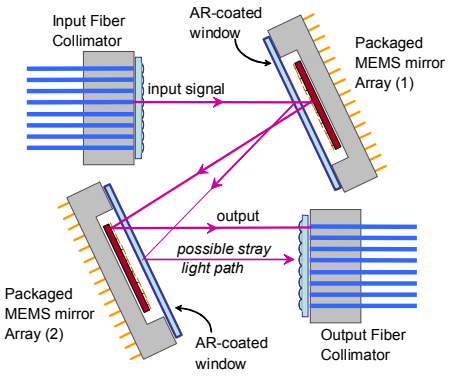

Fig. 1 Schematic of a representative MEMS optical switch, showing a typical signal path through 8 surfaces of the AR-coated windows, and one possible noise path from unwanted hermetic sealing window reflections.

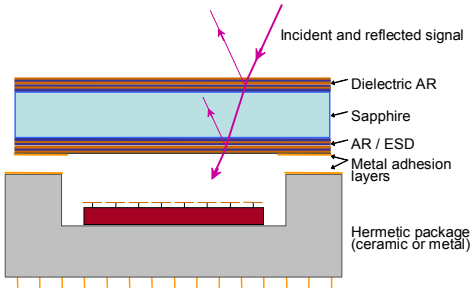

Fig. 2 Schematic of a hermetic package for an optical MEMS device, showing electrical attachment of the conductive AR-coated window to the ceramic chip carrier by solder or brazing.

operation of the device. Second, this same surface charge will attract dust particles and, in time, the accumulated dirt will affect the transparency of the window. For this reason, the window surface in contact with the metallic casing should carry an electrically conducting AR coating so that the charge can be dissipated (Fig. 2).

Indium Tin Oxide (ITO) is frequently used as a transparent conductive coating for visible light applications, and a sufficiently thin (~0.5 micron) layer is also usable for the near infrared wavelengths. However, the optical properties of ITO change under annealing [3] and an initially transparent film (>95% transmittance) can become relatively absorptive (10 – 20% absorptance) following sustained heating. Continuous optical power densities in telecommunications applications are substantial (i.e., 100 mW in a 10 micron mode field diameter is 127 kW/cm^2) and even a small initial absorption can lead to localized heating which results in higher absorption in the ITO coating. ITO films also suffer from substantial PDL with off-axis illumination. For these reasons, improved near-IR conducting AR coatings are needed which can be fabricated with conventional materials and tools.

In Section 2 of this paper the design of conducting AR coatings for the 1200-1630 nm spectral region that are effective for angles of incidence up to 38° are described. Because all conducting coatings for this region of the wavelength spectrum exhibit some transmission losses, non-absorbing all-dielectric coatings with otherwise similar performance characteristics have also been designed in order to reduce the combined losses of a window (Section 3). In Section 4 it is shown that conducting AR coatings can also be designed based on other coating materials or for larger angular ranges. In Section 5, the manufacture of a prototype AR coating is described along with a comparison of the measured and theoretical results. Finally, some conclusions are presented in Section 6.

2. Conducting AR coating designs for $0<\theta<38^{o}$

For the AR coatings described in this Section, an additional requirement was that the surface of the coating be conducting, with a sheet resistivity less than 10 MΩ/□. Such a resistivity was deemed necessary for any charges that build up on the surface of the coating to be readily discharged to the metallic housing to which it is attached to form a hermetic seal.

Thelen wrote one of the earliest papers on transparent conducting AR coatings [4]. Since these type of coatings find applications, for example, in computer monitors, TV tubes, and lenses for video projection, it is not surprising that many more papers and patents have been published on this topic since those early days. Here we cite only a few of these [5-7]. The most commonly used transparent conducting material is indium tin oxide (ITO) but others, like doped SnO_2 and Al_2O_3 and Cd_2SnO_4, have also been used in the visible part of the spectrum. Transparent conducting coatings for the infrared usually consist of thin metallic layers, such as Au, Ag, Ni, Kovar, Inconel or of Ge, Si and other materials from the III-V group of semiconductors.

Unfortunately, all transparent conducting coatings give rise to some absorption losses in the near-IR wavelength range of interest. This is usually not much of an issue in the applications in which the light passes through the conducting AR coating only once. However, as stated above, in devices such as MEMS optical switches, the beam may have to pass through a window as many as four times, and under such conditions even small losses accumulate rapidly. Certainly, transparent metallic layers have to be ruled out for this application. The performance of some initial conducting AR coating designs based on ITO was quite unacceptable: for the required thickness, the ITO had significant absorption at wavelengths greater than 1000 nm leading to unacceptable losses of the order of 3.0 dB after eight passes through the ITO based coating.

The conductive AR coating solutions presented here are all based on a ~10 nm thick silicon (Si) layer capped by a 2 nm thick native oxide layer that does not materially affect the conductance yet protects the Si layer from further oxidation. The use of a Si layer in a conducting AR coating was not obvious for two reasons. First, this material is opaque in the

visible and slightly absorbtive in the near-IR. Second, it has a quite high refractive index and placing such a layer at the air interface of an AR coating is counter-intuitive. However, such a layer pair can have a sheet resistivity of less than 10 MΩ/□. More details on the manufacture and properties of such a conducting coating will be given in Section 5.

The numerical solutions described below were all found with the proprietary thin film design software TF*Architect* developed at the NRCC. This is a Windows version of the DOS program TF*Design* described at length in reference [8]. The main optical performance targets for both the conducting and non-conducting AR coatings used in most of the calculations were as follows. The transmittance T_S and the PDL_T were both specified to be 0.0 dB with tolerances of 0.02 and 0.007 dB, respectively, for 21 equi-spaced wavelengths λ in the 1200-1620 nm spectral region and for six angles of incidence θ: 0, 10, 20, 30, 35 and 38°. On a linear scale, this corresponds to T_S=1.00 and T_s/T_p=1.000 with tolerances of 0.005 and 0.002, respectively. The numerical calculations were therefore driven by a merit function M (using a dB scale) defined in the following way:

$$M = \left\{ \frac{1}{126} \sum_{\theta=1}^{6} \sum_{\lambda=1}^{21} \left[\left(\frac{0.00 - (T_s)_{\lambda,\theta}}{0.02} \right)^2 + \left(\frac{0.00 - PDL_{\lambda,\theta}}{0.007} \right)^2 \right] \right\}^{0.5} \qquad (1)$$

Clearly, with these tolerances, the PDL_T specifications are given considerably more weight than the transmittance specifications. Unless otherwise stated, all solutions that are described in this paper are based on the use of a thin Si conducting layer, a sapphire substrate and SiO_2 and Nb_2O_5 thin film dielectric layers. These latter are standard coating materials

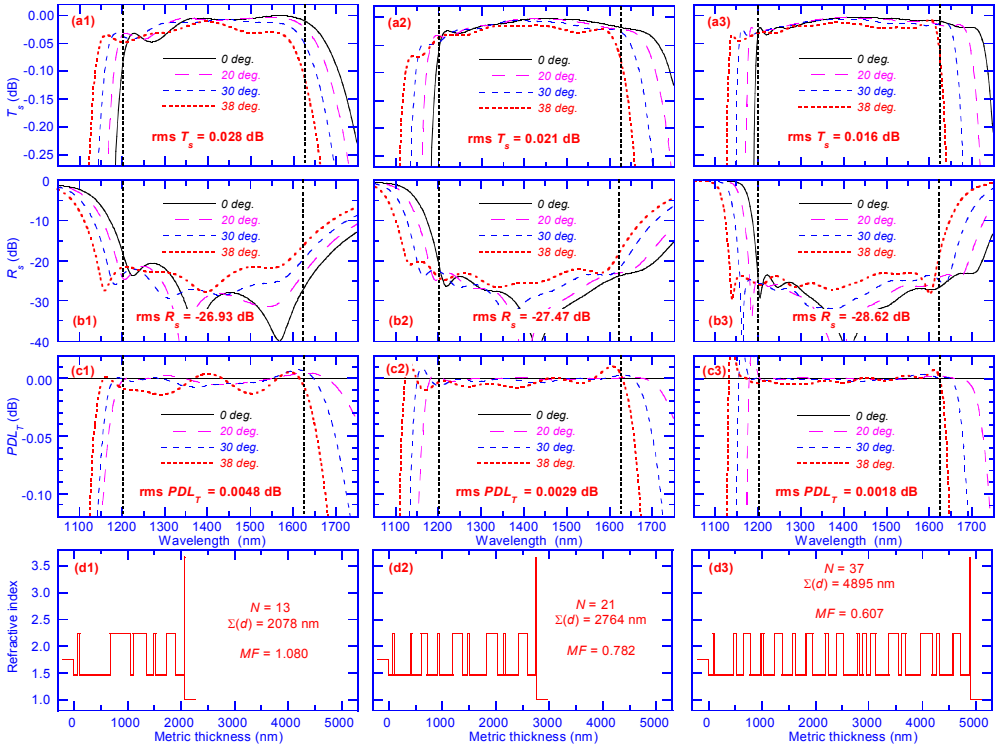

Fig. 3. Calculated values of T_S, R_S, and PDL_T (rows a-c) for different angles of incidence and refractive index profiles (row d) for three different conducting AR coatings (columns 1-3)

that can be deposited by different methods including e-gun evaporation, ion plating, ion beam plating, as well as RF- and AC magnetron sputtering. Both SiO_2 and Nb_2O_5 layers are very stable and mechanically robust.

The refractive index profiles and calculated performances of three different conducting AR coatings designed on this basis are depicted in Fig. 3. The diagrams in columns 1, 2 and 3 correspond to solutions with progressively increasing overall total thickness and number of layers. The spectral transmittances T_S of the three systems are shown in row (a). For clarity, the data is plotted only for angles of incidence of 0, 20, 30 and 38°. Since conducting coatings have a non-zero absorptance, $T+R\neq1.0$, it was deemed desirable also to present the calculated reflectance R_S in row (b). Similar information for the PDL_T is provided in row (c). The calculated *rms* values of T_S, R_S and PDL_T (expressed in dB) for all the combinations of wavelengths and angles of incidence which contributed to the merit function (Eq. (1)) are also given in the diagrams of rows (a), (b), and (c). In all the above diagrams the spectral region over which the performance is optimized is indicated by two vertical dotted lines. Finally, the refractive index profiles, the number of layers, the total metric thicknesses and the calculated merit functions *MF* of the systems are shown in the diagrams of row (d). The metric thicknesses of the individual layers of the three solutions, together with the other numerical data presented in Fig. 3, are also listed in Table 1.

Despite the use of a layer with a high refractive index at the AR/air interface, the calculated performances of the AR coatings are quite impressive. As expected, with an increasing number of layers and overall thickness, the performance of the AR coatings is improved. The calculated performance of the system of Fig. 3 (c3) meets the specifications.

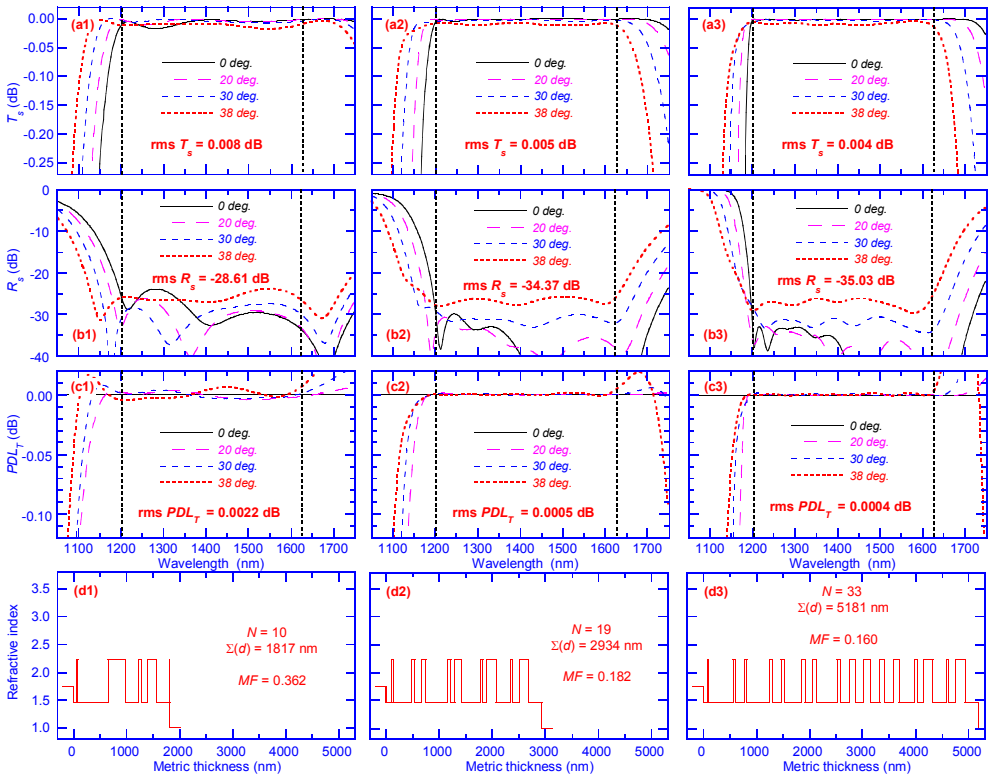

Fig. 4. Calculated values of T_s, R_s, and PDL_T (rows a-c) for different angles of incidence and refractive index profiles (row d) for three different non-conducting AR coatings (columns 1-3)

Table 1. Construction parameters and some properties of the layer systems

	Fig.3, col.1		Fig.3, col.2		Fig.3, col.3		Fig.4, col.3		Fig.4, col.2		Fig.4, col.1		Fig.6, col.1		Fig.6, col.2	
No.	N	d (nm)	n	d (nm)	n	d (nm)	n	d (nm)	n	d (nm)	n	d (nm)	n	d (nm)	n	d (nm)
subs.	1.747		1.747		1.747		1.747		1.747		1.747		1.747		1.747	
1	1.462	64.94	1.462	75.16	1.462	92.22	1.462	90.18	1.462	119.77	1.462	56.65	1.397	57.06	1.462	99.38
2	2.227	42.59	2.227	35.51	2.227	27.89	2.227	18.41	2.227	20.22	2.227	33.46	2.227	42.16	2.227	28.99
3	1.462	577.94	1.462	292.78	1.462	358.64	1.462	465.82	1.462	348.91	1.462	562.99	1.397	583.24	1.462	340.36
4	2.227	376.10	2.227	38.24	2.227	48.47	2.227	44.20	2.227	62.83	2.227	328.12	2.227	350.43	2.227	46.14
5	1.462	54.65	1.462	167.93	1.462	124.08	1.462	159.14	1.462	125.82	1.462	247.99	1.397	70.33	1.462	139.18
6	2.227	242.99	2.227	109.20	2.227	130.95	2.227	45.40	2.227	78.23	2.227	50.01	2.227	317.70	2.227	135.64
7	1.462	126.89	1.462	201.85	1.462	209.40	1.462	428.15	1.462	406.08	1.462	111.23	1.397	144.88	1.462	168.74
8	2.227	51.66	2.227	27.25	2.227	48.11	2.227	49.50	2.227	62.50	2.227	173.01	2.227	49.33	2.227	56.20
9	1.462	201.27	1.462	253.27	1.462	195.85	1.462	166.63	1.462	77.85	1.462	252.66	1.397	158.44	1.462	248.78
10	2.227	162.35	2.227	184.86	2.227	142.54	2.227	59.26	2.227	128.65	2.227	0.70	2.227	156.37	2.227	107.68
11	1.462	165.03	1.462	91.75	1.462	196.35	1.462	317.71	1.462	352.44			1.397	165.64	1.462	191.25
12	3.656	10.00	2.227	34.14	2.227	59.14	2.227	73.24	2.227	47.39			3.656	10.00	2.227	55.12
13	1.462	2.00	1.462	323.93	1.462	182.33	1.462	148.99	1.462	69.28			1.462	2.00	1.462	237.91
14			2.227	198.14	2.227	138.59	2.227	67.61	2.227	179.54					2.227	140.04
15			1.462	106.39	1.462	235.23	1.462	391.40	1.462	273.92					1.462	155.01
16			2.227	41.05	2.227	64.37	2.227	65.67	2.227	31.45					2.227	47.67
17			1.462	255.02	1.462	141.15	1.462	163.99	1.462	123.58					1.462	285.21
18			2.227	153.38	2.227	133.96	2.227	107.41	2.227	179.77					2.227	137.88
19			1.462	162.54	1.462	258.36	1.462	153.05	1.462	245.91					1.462	147.12
20			3.656	10.00	2.227	40.24	2.227	132.86							2.227	42.90
21			1.462	2.00	1.462	59.59	1.462	178.93							1.462	274.83
22					2.227	71.31	2.227	89.34							2.227	183.90
23					1.462	70.38	1.462	162.67							1.462	92.96
24					2.227	103.49	2.227	109.69							2.227	34.45
25					1.462	244.04	1.462	291.79							1.462	325.93
26					2.227	191.33	2.227	56.89							2.227	221.56
27					1.462	42.49	1.462	111.75							1.462	110.14
28					2.227	77.86	2.227	175.40							2.227	27.30
29					1.462	283.28	1.462	250.97							1.462	289.93
30					2.227	213.63	2.227	38.18							2.227	153.90
31					1.462	82.63	1.462	139.19							1.462	167.97
32					2.227	46.62	2.227	175.64							3.656	10.00
33					1.462	253.98	1.462	251.68							1.462	2.00
34					2.227	151.76										
35					1.462	162.28										
36					3.656	10.00										
37					1.462	2.00										
air	1.000		1.000		1.000		1.000		1.000		1.000		1.000		1.000	

Σd	2078.41	2764.39	4894.57	5180.75	2934.12	1816.81	2107.59	4706.04
MF	1.080	0.782	0.607	0.160	0.182	0.362	0.894	1.630
RMS Ts	0.0275	0.0206	0.0164	0.0044	0.0050	0.0081	0.0223	0.0452
RMS Rs	-26.93	-27.470	-28.616	-35.031	-34.368	-28.605	-27.704	-26.077
RMS PDL	0.0048	0.0029	0.0018	0.0004	0.0005	0.0022	0.0042	0.0037

3. Non-conducting AR coating designs for $0<\theta<38^{o}$

As stated above, only one of the AR coatings on the sapphire window needs to be conducting. The overall performance of the window would be improved if the second AR coating were to be made entirely out of dielectric materials. In Fig. 4 are shown the calculated performances and refractive index profiles of three such systems. For easier comparison, the data in this diagram is presented in the same way as in Fig. 3. These results were derived from the systems of Fig. 3, by removing the capping SiO_2 layer and by replacing the Si layer by a Nb_2O_5 layer. Each system was then refined. It will be seen that in the refinement process the thicknesses of the layers were considerably modified, the total number of layers was changed, and that, in two cases, the thin high refractive index Nb_2O_5 layers at the air interface were removed (see Table 1). Not surprisingly in each instance the transmittance losses were reduced over those for the corresponding conducting coatings. It will also be seen from this diagram that there is little gain in performance by increasing the number of layers of the system from 19 to 33.

Figure 5 illustrates the significance of using different AR coatings on the two sides of four otherwise identical sapphire windows. Columns 1 and 2 show the calculated T_S and PDL_T values for one and for four-coated windows. The graphs in row (a) correspond to substrates in which identical conducting AR coatings of the 37-layer design depicted in graph c3 of Fig. 3 are applied to all surfaces. In this figure all the T_S and PDL_T values shown correspond to an angle of incidence of 38º. In the graphs in row (b), all AR coatings correspond to the 19-layer non-conducting design of graph c2 of Fig. 4. This of course is not an option since one of the AR coatings on each window must be conducting, but the results are presented here for comparison purposes. The graphs in row (c) assume that one side of each window is coated with the design of graph c3 of Fig. 3, and the other side with the design of graph c2 of Fig. 4. Clearly, for best results, conducting and non-conducting AR coatings should be combined - this is the preferred option.

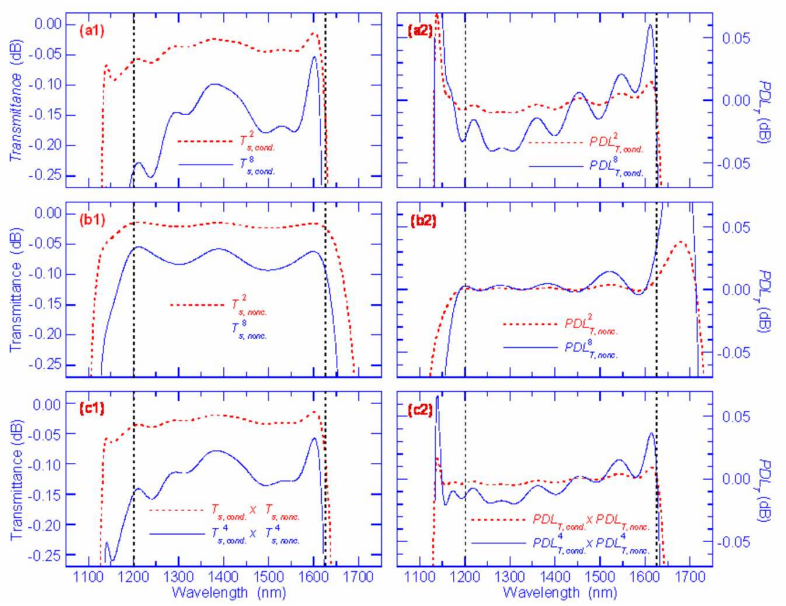

Fig. 5. Calculated T_s, PDL_T values (columns 1, 2) for 38º incidence of four windows placed in series, each with two AR-coated surfaces: row a – two conducting ARs of Fig. 3 d3; row b – two non-conducting ARs of Fig. 4 d2; row c – one conducting and one non-conducting AR.

4. Other conducting AR coating designs

In this Section we present two additional examples to illustrate the fact that conducting AR coatings with a similar performance can also be designed for other specifications and that solutions can be found that are based on other coating materials.

All the AR coatings described thus far have essentially been based on the use of SiO_2 and Nb_2O_5 layers. Of course, other materials could also have been used. The specifications for the example depicted in column 1 of Fig. 6 are exactly the same as those for the systems depicted in Fig. 3. However, this time the design is based on ZnS and MgF_2, materials that can be readily evaporated from resistance-heated sources or by electron beam guns. Such a process might lend itself to larger area coatings, provided that it can be sufficiently well controlled. The conducting Si layer and its native oxide layer are the same as in the other designs. It will be seen from this figure that the calculated performance of this system is, if anything, somewhat better than that of the Nb_2O_5/SiO_2 system of comparable thickness and number of layers. This is due to the fact that the refractive index of MgF_2 is lower than that of SiO_2.

The next design was based on the same AR specifications as before except now the angle of incidence range was extended to 55º. In column 2 of Fig. 6 are shown the calculated results for a conducting AR coating made of the same materials that were used in the design of the systems depicted in Fig. 3. Not surprisingly, it can be seen from Fig. 6 that although

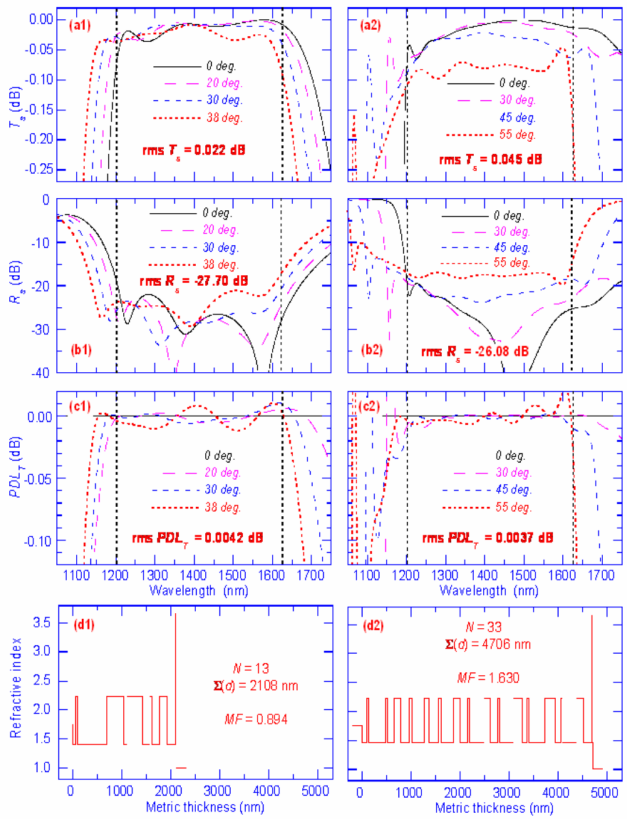

Fig. 6 Calculated values of T_s, R_s, PDL_T (rows a-c) for different angles of incidence θ and refractive index profiles (row d) for two additional conducting AR coatings: column 1–AR coating based on ZnS and MgF_2 coating materials; column 2 –AR coating designed for angles of incidence $0< \theta <55º$.

the calculated results for the solution found are still quite good, extending the angle of incidence range has somewhat compromised the performance.

5. Manufacture and experimental results

Before proceeding to the manufacture of a multilayer it is always prudent to carry out an error analysis to see if the system is sensitive to errors in the layer thicknesses or refractive indices. Reasonable thickness errors correspond to 1% of a layer's thickness for thicker layers and up to a maximum of 1 nm for thinner layers. For this reason we have carried out, for each of the systems depicted in Fig. 3, two sets of 50 calculations on systems in which the individual layers were randomly perturbed with thickness errors not exceeding 1% and 1 nm, respectively. The calculations were performed at an angle of incidence of 38º, the most critical case. In Fig. 7, rows (a)-(c) correspond to the results for the three different systems and in columns 1 and 2 are plotted the upper and lower envelopes for T_S and PDL_T curves within which one would expect the performance of 66% of the AR coatings manufactured with the above type of thickness error to fall. From these curves one can conclude that the chances of successfully manufacturing these coatings are good. An analysis of the effect of random errors in the thin film refractive indices was not performed because layer-to-layer reproducibility of the optical constants is very good for the deposition process proposed for the manufacture of the coatings.

A similar set of calculations on the 19-layer system of Fig. 4 (d2) shows that the sensitivity to thickness errors of the non-conducting AR coatings is smaller than that of the conducting AR coatings. This is not surprising as a 1 nm thickness error in the Si layer in the conducting coatings represents a 10% change in the thickness of that layer which, in turn, has a significant effect on the absorption of the system. This problem does not exist in the non-conducting AR coatings.

The 37-layer system shown in Fig. 3, column 3 was selected to be manufactured as it provides a very good conducting AR performance. This coating was deposited on an AC magnetron sputtering system similar to the one described in reference [9]. The same system was also used for the manufacture of the Iridian entry to the Manufacturing Problem at the 2001 Topical Meeting on Optical Interference Coatings in Banff [10]. The interested reader is

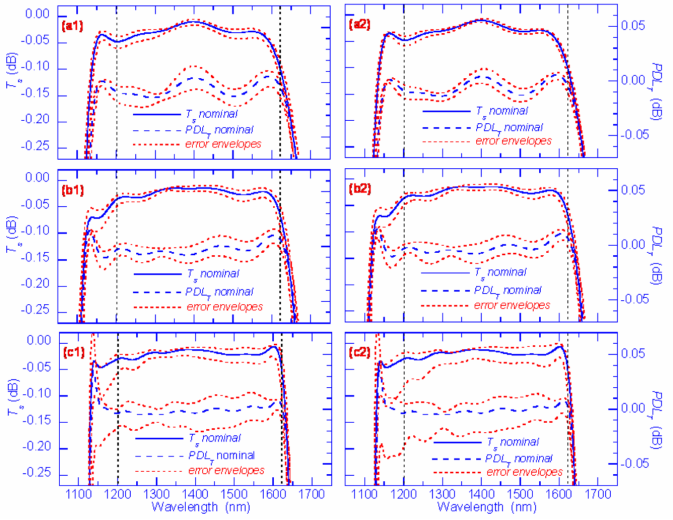

Fig. 7. Sensitivity of the calculated values of T_s, and PDL_T for 38º incidence of the conducting AR coatings of Fig. 3 (rows a-c) to 1% and 1 nm random errors (columns 1, 2) in the layer thicknesses (see text for details)

referred to these two papers for more detail on the deposition system and process control used for manufacturing the prototype conducting AR coating. Here we will only state that *in-situ* measurements were made to determine layer thicknesses accurately while real-time re-optimization was used to minimize the effects of small thickness errors that occurred during the deposition of the individual layers.

The deposition of the (amorphous) Si layer posed some unique challenges. It is important to purge the deposition chamber of any oxygen during deposition to avoid the Si layer oxidizing during deposition but it is also necessary to expose the Si layer to atomic oxygen after deposition in order to stabilize and protect the Si layer. Therefore, after depositing the oxide layers, the oxygen flow was stopped and the Si targets were pre-sputtered in an argon only plasma until the oxide layer was removed from the Si targets. The Si layer was then deposited after which oxygen was re-introduced into the chamber and the Si layer was oxidized forming a ~2 nm protective oxide layer. Note that the Si layer was deposited with a thickness that took into account the amount of material that would be oxidized during the formation of the protective oxide layer. More information on the protection of thin metal layers from oxidation will be found in Ref. [11].

For the prototype conducting AR-coated window, the same conducting AR coating was deposited on both sides of a c-axis sapphire crystal. A monitor slide of BK7 was used in the AR coating runs for the *in-situ* measurements. Figure 8 shows that there is good agreement between the transmission measurements of the completed AR systems taken *in-situ* on the monitoring slides and the calculated transmittances based on the determination of the individual layers during the deposition. Further, the results are almost exactly the same for the AR coatings on both sides. The deposition process is therefore very predictable and repeatable. The transmittance measurements were made on a Perkin-Elmer UV/VIS/NIR Lambda 19 spectrophotometer.

Figure 9 shows the transmittance of a bare sapphire substrate and the prototype conducting AR coated sapphire window at normal incidence along with the theoretical desired and calculated transmittance curves. As can be seen there is good agreement between the desired and the calculated transmittance curves, where the calculated curve is based on the layer thicknesses determined during the deposition run. The difference between the measured and desired theoretical curves is within 1.2% which implies that for a single conducting AR coating, the difference between desired and measured is around 0.6%.

To look at the Si layer absorption, Fig. 10 shows the near-normal transmittance and reflectance of the prototype conducting AR coated window along with their sum. Within the measurement accuracy there appears to be no significant amount of absorption in the layer system in the spectral range of interest.

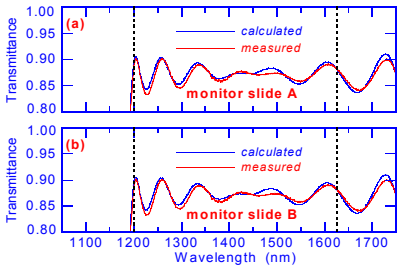

Fig. 8. Monitoring precision for an experimental conducting AR coating of the type depicted in column 3 of Fig. 3. Figures a and b compare the calculated and the measured *in-situ* transmittances of monitoring slides for the AR coatings deposited on sides A and B

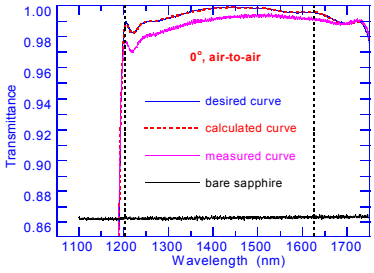

Fig. 9. Comparison of the measured normal incidence transmittances of a substrate with the target transmittance and the transmittance calculated from the thicknesses of the layers determined during the deposition. In this and subsequent diagrams, the two sides of each substrate carry the same conducting AR coating.

The transmittance of the prototype conducting AR coated window was measured using a swept laser system for an angle of incidence of 40° over the 1540 to 1620 nm wavelength region for un-polarized and p-polarized light (Fig. 11). Within this wavelength region, the measured and calculated transmittance curves are within 1% of each other and, as well, the p-polarized and un-polarized data are in good agreement with each other indicating that the PDL of these coatings is low.

To test the conductivity of the AR coating it is necessary to make an ohmic contact with the 10 nm thick amorphous Si layer. Attempts to measure conductivity with a conventional four-point probe were unsuccessful, apparently because the probe tips would fracture the Si layer. Proper measurement of conductivity requires evaporation of suitably thick (100 – 200 nm thick) and separate metal onto the Si layer, preferably immediately after the Si layer is deposited and before the protective oxide layer is formed. We expect that this coating will be at least somewhat sensitive to environmental effects, as exposure of the early samples to water slightly decreased the transmission. The best procedure for forming ohmic contact to the conducting layer, and the effects of environmental exposure to the thin Si layer, will be the subject of a follow-on study. It is worth noting that the intended application of this window for hermetic and antistatic sealing of MEMS devices (as shown in Figure 1) requires a conductive layer only in the controlled environment of the interior of the hermetically-sealed package. The outer layer required low reflectivity and PDL, but does not incorporate the conducting Si layer.

6. Conclusions

It has been shown in this paper that, using conventional coating materials, it is possible to design AR coatings that are effective both over a fairly broad spectral region ($\lambda_{long}/\lambda_{short} \approx 1.40$) and a wide range of angles of incidence (0-38º, or even 0-55º). Not only is the theoretical transmittance of windows treated with such coatings quite high, but they also have very good polarization independence (low PDL_T values).

The coatings can incorporate a thin amorphous Si upper layer which should provide a conductive surface of approximately 10MΩ/□ sheet resistivity. Despite the high refractive index of this layer, is was possible to generate designs without significant impact on the transmittance over the 1200-1630 nm design wavelength, such that low optical loss components using multiple passes through the window become practical. When windows with conducting AR coatings are attached to a metallic housing, they can protect the contents from electrostatic fields and prevent the attraction of dust particles. This should be of interest in the construction of MEMS. If the conducting AR systems are made predominantly of oxide layers, it should be possible to make robust brazed connections to the metallic housing. The range of coating materials can be expanded if a lower temperature bonding process, such as conducting cement, is used.

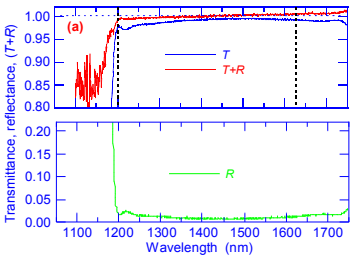

Fig. 10 Measured normal incidence transmittance T, reflectance R and the sum (T+R).

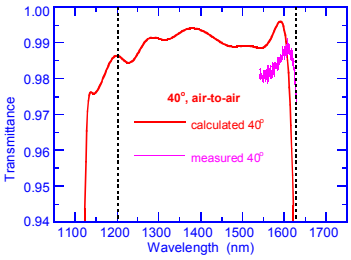

Fig. 11 Comparison of the calculated and measured transmittance for unpolarized and p-polarized light incident at 40˚ of an AR coating prepared during run 3.

As in most optical thin film problems, the performance of the AR coatings depends on the overall optical thickness and the number of layers in the system. In this paper, examples were given of coatings consisting of up to 37 layers. If a better performance was required and if economic considerations were to permit it, this number could readily be expanded to more than 60 layers. All the AR coatings discussed in this paper were designed for sapphire substrates but there are no reasons why similar coatings could not be produced for other window materials such as Si, fused quartz and various specialty glasses. Further, it should be possible to design similar coatings for other spectral regions although the Si layer might have to be replaced by a different conducting material that has a small extinction coefficient at the chosen wavelengths.

One of the designs, depicted in Fig. 3 (d3), was produced experimentally and its measured optical performance was in reasonable agreement with the calculated curves for both unpolarized and p-polarized light. With further work, it should be possible to achieve an even better agreement between the desired and measured performance. It was not possible to measure the sheet resistance of the sample using conventional four-point probe methods. A procedure for forming ohmic contact to the conducting layer, and the effects of environmental exposure to the thin Si layer, will be the subject of another paper.

Acknowledgments

The authors would like to thank Dr. Penghui Ma for suggesting that thin Si layers might have a suitable sheet resistance and that the native oxide on their surface would protect them from further oxidation.